



## Paleoceanography

### RESEARCH ARTICLE

10.1002/2016PA003053

#### Key Points:

- Shallow subsurface reservoir ages were about 1500 years during the late glacial period at 26 ka
- During Heinrich Stadial 1, *Pyrgo* species date up to 7000 years older than coeval perforate benthic foraminiferal species
- Ventilation and surface-deep mixing in the Nordic Seas, likely indicative of overturning, were suppressed during cold periods

#### Supporting Information:

- Supporting Information S1

#### Correspondence to:

M. M. Ezat,  
mohamed.ezat@uit.no

#### Citation:

Ezat, M. M., T. L. Rasmussen, D. J. R. Thornalley, J. Olsen, L. C. Skinner, B. Hönisch, and J. Groeneveld (2017), Ventilation history of Nordic Seas overflows during the last (de)glacial period revealed by species-specific benthic foraminiferal  $^{14}\text{C}$  dates, *Paleoceanography*, 32, doi:10.1002/2016PA003053.

Received 12 NOV 2016

Accepted 3 FEB 2017

Accepted article online 10 FEB 2017

## Ventilation history of Nordic Seas overflows during the last (de)glacial period revealed by species-specific benthic foraminiferal $^{14}\text{C}$ dates

Mohamed M. Ezat<sup>1,2</sup> , Tine L. Rasmussen<sup>1</sup> , David J. R. Thornalley<sup>3</sup> , Jesper Olsen<sup>4</sup> , Luke C. Skinner<sup>5</sup>, Bärbel Hönisch<sup>6</sup> , and Jeroen Groeneveld<sup>7</sup> 

<sup>1</sup>Centre for Arctic Gas Hydrate, Environment and Climate, Department of Geosciences, UiT, The Arctic University of Norway, Tromsø, Norway, <sup>2</sup>Department of Geology, Faculty of Science, Beni-Suef University, Beni-Suef, Egypt, <sup>3</sup>Department of Geography, University College London, London, UK, <sup>4</sup>Department of Physics and Astronomy, Aarhus University, Aarhus, Denmark, <sup>5</sup>Godwin Laboratory for Palaeoclimate Research, Department of Earth Sciences, University of Cambridge, Cambridge, UK, <sup>6</sup>Department of Earth and Environmental Sciences, Lamont-Doherty Earth Observatory, Columbia University, Palisades, New York, USA, <sup>7</sup>Center for Marine Environmental Sciences (MARUM), University of Bremen, Bremen, Germany

**Abstract** Formation of deep water in the high-latitude North Atlantic is important for the global meridional ocean circulation, and its variability in the past may have played an important role in regional and global climate change. Here we study ocean circulation associated with the last (de)glacial period, using water-column radiocarbon age reconstructions in the Faroe-Shetland Channel, southeastern Norwegian Sea, and from the Iceland Basin, central North Atlantic. The presence of tephra layer Faroe Marine Ash Zone II, dated to ~26.7 ka, enables us to determine that the middepth (1179 m water depth) and shallow subsurface reservoir ages were ~1500 and 1100  $^{14}\text{C}$  years, respectively, older during the late glacial period compared to modern, suggesting substantial suppression of the overturning circulation in the Nordic Seas. During the late Last Glacial Maximum and the onset of deglaciation (~20–18 ka), Nordic Seas overflow was weak but active. During the early deglaciation (~17.5–14.5 ka), our data reveal large differences between  $^{14}\text{C}$  ventilation ages that are derived from dating different benthic foraminiferal species: *Pyrgo* and other miliolid species yield ventilation ages >6000  $^{14}\text{C}$  years, while all other species reveal ventilation ages <2000  $^{14}\text{C}$  years. These data either suggest subcentennial, regional, circulation changes or that miliolid-based  $^{14}\text{C}$  ages are biased due to taphonomic or vital processes. Implications of each interpretation are discussed. Regardless of this “enigma,” the onset of the Bølling-Allerød interstadial (14.5 ka) is clearly marked by an increase in middepth Nordic Seas ventilation and the renewal of a stronger overflow.

### 1. Introduction

Terrestrial and marine sediment records document that the last deglaciation (~19–10 ka) was interrupted by two climatic anomalies, Heinrich Stadial (HS) 1 and the Younger Dryas (YD) stadial, which were characterized by cooling over Greenland, warming of the Antarctic region, global net warming, and rise in atmospheric  $\text{CO}_2$  [Dansgaard et al., 1993; European Project for Ice Coring in Antarctica, 2006; Shakun et al., 2012; Monnin et al., 2001]. Large-scale reorganizations of the Atlantic Meridional Overturning Circulation (AMOC) are thought to be a key player in these climate anomalies, through direct and indirect modulation of global heat distribution [Broecker, 1998], air-sea  $\text{CO}_2$  exchange, and the efficiency of nutrient utilization [Sigman and Boyle, 2000; Skinner et al., 2014]. In the modern ocean, poleward advection of warm and salty Atlantic water across the Greenland-Scotland Ridge (GSR) into the Nordic Seas and Arctic Ocean, where it densifies and overflows the GSR to the North Atlantic, contributes to the lower North Atlantic Deep Water, an important component of the AMOC [Hansen and Østerhus, 2000].

Ocean circulation and air-sea gas exchange can be inferred from radiocarbon ventilation ages, which are defined as the ocean-atmosphere radiocarbon isotope disequilibrium [e.g., Soulet et al., 2016] and which are therefore broadly indicative of the time since the water was last in contact with the atmosphere. This ocean-atmosphere radiocarbon isotope disequilibrium responds to changes in rate of water renewal, air-sea gas exchange, sources of water masses, and mixing. The deepwater formation in the Nordic Seas via open ocean convection [Hansen and Østerhus, 2000], gradual transformation of Atlantic water [Eldevik et al., 2009], and seawater freezing and salt rejection [Mauritzen, 1996] results in well-ventilated overflow waters to the North Atlantic (ventilation age of ~500 years) and a minimal surface-deep seawater age offset (~100 years)

[Broecker and Peng, 1982]. To constrain past variations in the North Atlantic circulation and its interaction with climate during the Last Glacial Maximum (LGM) and deglaciation, several studies have applied  $^{14}\text{C}$  measurements in planktic and benthic foraminifera to infer changes in regional water column ventilation [Skinner and Shackleton, 2004; Sarnthein et al., 2007; Thornalley et al., 2011, 2015; Stern and Lisiecki, 2013; Skinner et al., 2014].

In contrast to the modern situation, reconstructions of  $^{14}\text{C}$  ventilation ages from south of Iceland during HS1 and YD show extremely old ages (up to 5000  $^{14}\text{C}$  years) and were tentatively attributed to venting of an aged reservoir in the deep Southern Ocean and northward transport via the Antarctic Intermediate Water (AAIW) [Thornalley et al., 2011]. Subsequent studies from the South Atlantic reported deglacial ventilation ages for AAIW much younger than those recorded from south of Iceland, and thus do not support a southern source [Sortor and Lund, 2011; Cl  roux et al., 2011; Burke and Robinson, 2012]. More recently, Thornalley et al. [2015] provided evidence for the presence of extremely aged water in the deep Norwegian Sea (up to 10,000  $^{14}\text{C}$  years) during the last glacial, and they further suggested that episodic deglacial overflows from this aged reservoir may have been the source for the old ventilation ages recorded south of the Iceland rise [Thornalley et al., 2011]. If this scenario is correct, the signature of this aged overflow must be recorded in the Faroe-Shetland Channel, the main deep pathway of overflow water from the Norwegian Sea to the North Atlantic. We evaluate this hypothesis and study the North Atlantic-Norwegian Sea exchanges during the last glacial period (30–10 ka) based on radiocarbon measured in benthic and planktic foraminifera from core JM11-FI-19PC (62  49'N, 03  52'W, 1179 m water depth), in the Faroe-Shetland Channel, supplemented with species-specific benthic foraminiferal  $^{14}\text{C}$  dates from core RAPiD-10-1P (62  58'N, 17  35'W, 1237 m water depth) in the Iceland Basin (Figure 1).

## 2. Materials and Methods

### 2.1. Radiocarbon Analyses

For core JM11-FI-19PC, foraminiferal samples (5–12 mg) were  $^{14}\text{C}$  dated by accelerator mass spectrometry (AMS) at the  $^{14}\text{C}$ CHRONO Centre facility at Queen's University Belfast. Pretreatment of the foraminiferal samples followed the approach by Nadeau et al. [2001]. Samples were converted into graphite for AMS analysis on a Fe catalyst by using the hydrogen reduction method [Vogel et al., 1987]. Planktic radiocarbon ages are measured in the planktic foraminiferal species *Neogloboquadrina pachyderma*, which has a calcification depth range from ~30 to 200 m [e.g., Simstich et al., 2003]. Benthic radiocarbon ages are based on multispecies samples from the following infaunal benthic foraminifera: *Cassidulina neoteretis*, *Melonis barleeanus*, *Elphidium excavatum*, *Oridorsalis umbonatus*, and *Astrononion gallowayi* (hereafter the "infaunal benthic group"), which are the most abundant species (Figure S1 in the supporting information). Where possible, monospecific samples of epifaunal benthic species *Cibicidoides floridanus* (sometimes including specimens of *Cibicidoides* spp.) and the epifaunal to infaunal benthic species [Linke and Lutze, 1993] *Pyrgo serrata* (sometimes including specimens of *Pyrgo depressa* and other miliolid species) were radiocarbon dated from the HS1 interval. *Pyrgo* species are very rare or absent within our record, except for a small increase during HS1 (Figure S1).

For core RAPiD-10-1P, monospecific benthic foraminiferal samples, where possible, were picked from the >212  $\mu\text{m}$  size fraction from core RAPiD-10-1P for  $^{14}\text{C}$  analysis. Radiocarbon analyses were performed at National Ocean Sciences Accelerator Mass Spectrometry. No pretreatment was conducted other than examination under the microscope and removal of any obvious pieces of contamination.

### 2.2. Stable Isotope Analyses

Pristine specimens of *Pyrgo serrata* ( $N = 2$ –7; size fractions 250–500  $\mu\text{m}$  and/or >500  $\mu\text{m}$ ) and *Cibicidoides floridanus* and *Cibicidoides* spp. ( $N = 3$ –10; size fraction >150  $\mu\text{m}$ ) were picked for stable isotope analyses. The *Pyrgo serrata* analyses were performed at the Bjerknes Centre for Climate Research and the Department of Earth Sciences, University of Bergen, using a Finnigan MAT 253 mass spectrometer, whereas the *Cibicidoides* analyses were done at MARUM, University of Bremen, using a Finnigan MAT 251 mass spectrometer with an automated carbonate preparation device. The isotopic values are reported relative to the Vienna Peedee belemnite (VPDB), calibrated by using National Bureau of Standards (NBS) 18 and 19 (in addition to NBS 20 for the measurements at MARUM).

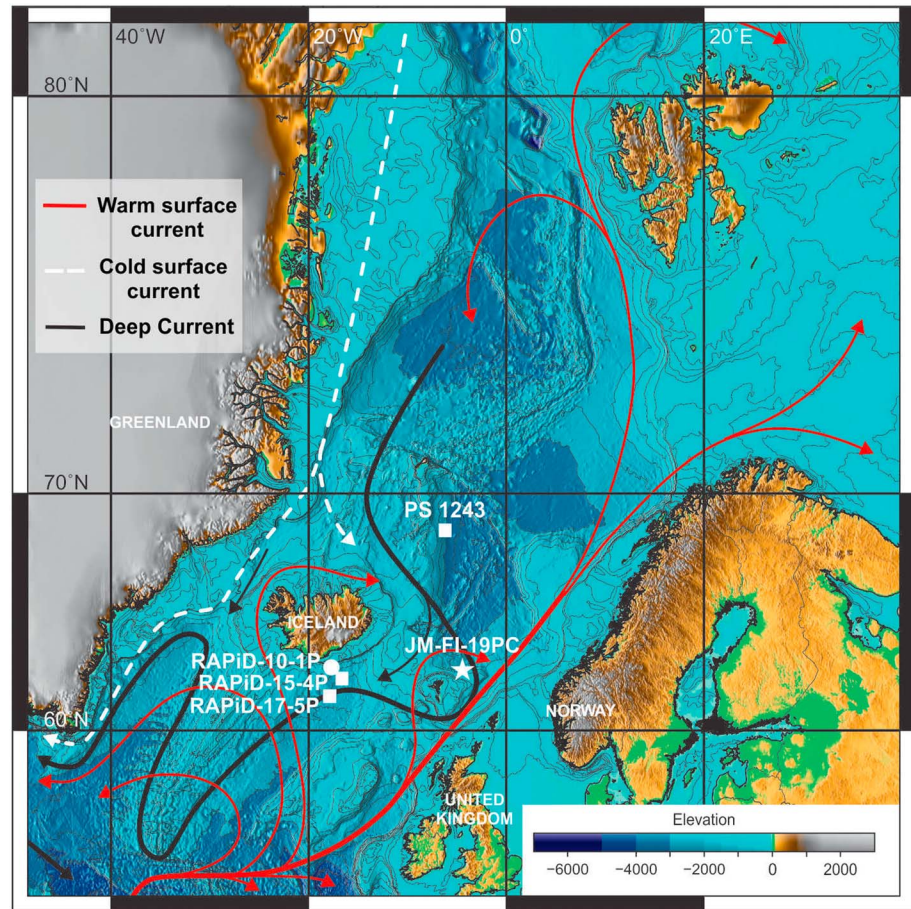


**Figure 1.** Map of major surface and bottom water currents in the northern North Atlantic and the Nordic Seas [Hansen and Østerhus, 2000]. Location of studied cores JM11-FI-19PC (1179 m water depth; star) and RAPiD-10-1P (1237 m water depth; circle) and other cores RAPiD-15-4P and RAPiD-17-5P (2133 and 2303 m water depth, respectively [Thornalley et al., 2011]) and PS1243 (2711 m water depth [Bauch et al., 2001; Thornalley et al., 2015]) (squares).

### 2.3. Age Models

The chronology for sediment core JM11-FI-19PC is based on alignment of tephra layers common in JM11-FI-19PC [Ezat et al., 2014] and the accurately dated Greenland ice cores [e.g., Svensson et al., 2008] as well as  $\delta^{18}\text{O}$  evidence for the onset of DO interstadials (IS) in Greenland ice cores [e.g., Svensson et al., 2008] and sharp increases in magnetic susceptibility and K/Ti measured by XRF scanning [Ezat et al., 2014] (see section 2 and Figure S1).

The Saksunarvatn tephra, Vedde ash, and Faroe Marine Ash Zone (FMAZ) II have been identified in JM11-FI-19PC by shards counting [Ezat et al., 2014] and by correlation to nearby core ENAM93-21 [see Hoff et al., 2016]. These tephra layers have been synchronized to their counterparts in the Greenland ice cores (dated 10.35, 12.17, and 26.74 ka, respectively [Davies et al., 2008; Svensson et al., 2008, and references therein]) and thus present marine-ice tie points. In addition, major and minor elemental analyses of FMAZ II in JM-FI-19PC proved that FMAZ II in JM11-FI-19PC is a well resolved primary deposit and can be used as a precise marine-ice isochron [Griggs et al., 2014]. Thus, the occurrence of this tephra layer provides confidence in our ventilation age reconstructions at this time.

In addition to the identified tephra layers, we used magnetic susceptibility, XRF-scanner K/Ti, and planktic and benthic foraminiferal  $\delta^{18}\text{O}$  to identify the onset of interstadials (IS) 1 and 2 in JM11-FI-19PC. The magnetic susceptibility from the region, which varies oppositely to K/Ti [see Richter et al., 2006; Ezat et al., 2014], has been proposed to reflect changes in the strength of deep currents transporting the magnetic particles from the source (the Icelandic volcanic province) to the site of deposition [Rasmussen et al., 1996; Kissel et al., 1999]. Ezat et al. [2014] identified IS1 in core JM11-FI-19PC at 190 cm core depth, when the magnetic susceptibility

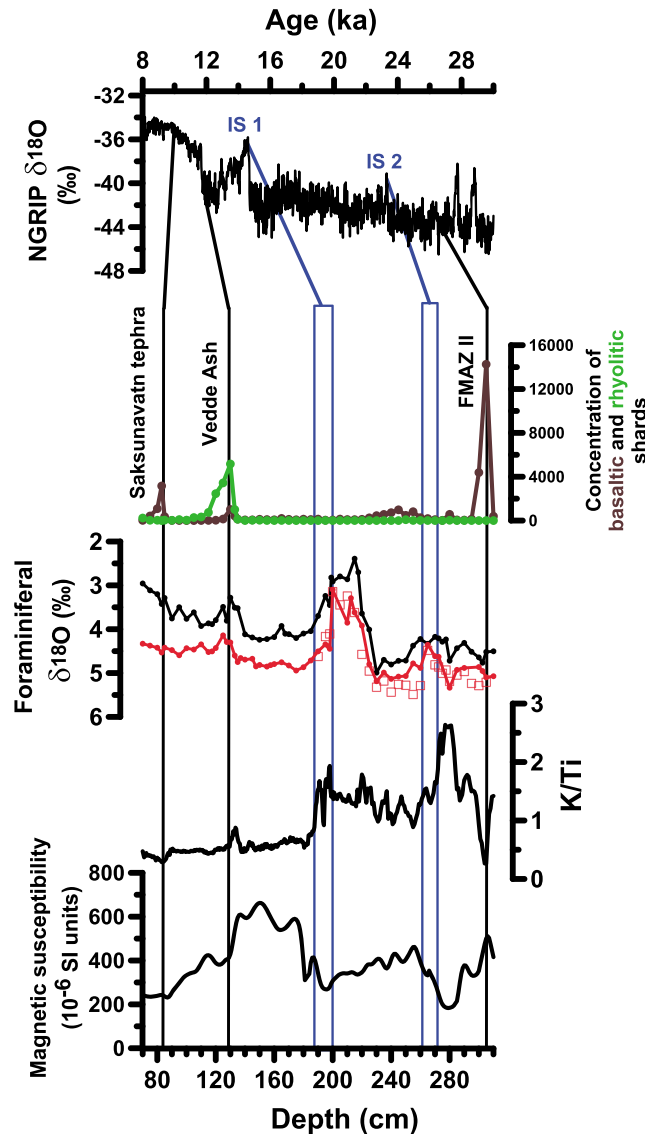


**Figure 2.** Correlation of core JM11-F1-19PC with Greenland ice cores based on location of tephra layers, magnetic susceptibility (MS), K/Ti, and benthic (red) and planktic (black)  $\delta^{18}\text{O}$ . The black lines refer to the locations of the tephra layers. The blue rectangles indicate a possible depth range for the onset of interstadials 1 and 2 based on correlation of the changes in MS, K/Ti, and foraminiferal  $\delta^{18}\text{O}$  with Greenland ice  $\delta^{18}\text{O}$ . Planktic  $\delta^{18}\text{O}$  data were measured in *Neogloboquadrina pachyderma* [Hoff et al., 2016], while benthic  $\delta^{18}\text{O}$  are measured in *Melonis barleeanus* (solid circles) and *Cassidulina neoteretis* (open squares) [Ezat et al., 2014]. Abbreviations: IS, interstadial; FMAZ, Faroe Marine Ash Zone. Greenland ice core data and tephra ages are from Svensson et al. [2008 and references therein].

*pachyderma*  $^{14}\text{C}$  age constraint (assuming a 400 year reservoir age) at the base of the sampled section at 410 cm of 18.8 ka.

#### 2.4. Ventilation Age Reconstructions

We reconstruct shallow subsurface (~100 m water depth) and bottom water  $^{14}\text{C}$  ventilation ages by comparing our planktic and benthic radiocarbon dates to contemporary atmospheric radiocarbon ages from Reimer et al. [2013] [cf. Skinner et al., 2010]. Additionally, we determine the age difference between the upper water

increased after HS1. However, the increase in magnetic susceptibility occurred very gradually from 197 to 190 cm core depth and there are two rapid decreases in K/Ti (at 195 and 190 cm core depth) (Figure 2). Instead, Hoff et al. [2016] and Ezat et al. [2016] used the large and abrupt increase in  $\delta^{18}\text{O}$  in benthic (~1‰) and planktic (~0.5‰) foraminifera at 197 cm core depth (Figure 2) as a marker of the onset of IS 1. The increase in benthic foraminiferal  $\delta^{18}\text{O}$  is thought to mark the end of HS1 and the onset of deep convection similar to today [e.g., Rasmussen and Thomsen, 2004; Meland et al., 2008]. Similarly, the change in magnetic susceptibility at the end of stadial 3 (beginning of IS 2) occurred gradually from 271 to 260 cm core depth, and there is a distinct decrease in K/Ti at 272 cm core depth (Figure 2). We therefore considered a range of possible scenarios of sediment depth-age model based on the available marine proxies (i.e., foraminiferal  $\delta^{18}\text{O}$ , magnetic susceptibility, and K/Ti) (Figure 2). In addition, the start of the deglacial  $\delta^{18}\text{O}$  decrease in *N. pachyderma* according to our age model is at ~17.5 ka [Hoff et al., 2016; Ezat et al., 2016], while it was dated ~16.5 ka according to the age model of Thornalley et al. [2015]. We also included this latter scenario (that is, the start of deglacial  $\delta^{18}\text{O}$  decrease in *N. pachyderma* could have occurred at 16.5 ka) in our possible range of calendar chronologies. This enables us to assess the influence of uncertainty in our calendar ages on the ventilation age reconstructions.

For sediment core RAPID-10-1P, we used the published age model for the past 17 kyr [Thornalley et al., 2010], with the addition of an *N.*

column and the bottom water by using the difference between paired benthic and planktic  $^{14}\text{C}$  dates. Hereafter, we will refer to radiocarbon ventilation ages as Plankton-Atmosphere (P-A) (that is, reservoir age "R" [Soulet *et al.*, 2016, and references therein]), Benthos-Atmosphere (B-A), and Benthos-Plankton (B-P) age offsets, all of which are taken strictly to reflect "relative isotopic enrichments," albeit expressed in equivalent radiocarbon years of isotopic decay [Soulet *et al.*, 2016; see also Cook and Keigwin, 2015]. We calculated the uncertainty in P-A and B-A ventilation ages based on the error propagation of uncertainty in foraminiferal  $^{14}\text{C}$  measurements and the atmospheric  $^{14}\text{C}$  record as well as the effect of uncertainty in age model (see section 2.3). The error propagation was calculated as the square root of the sum of the squared individual uncertainties. To calculate the associated uncertainties in B-P age offsets, we simply combined the errors in planktic and benthic  $^{14}\text{C}$  dates.

### 3. Results and Discussion

During the last glacial (at 26 ka), which is temporally well constrained in core JM11-FI-19PC by the presence of the Faroe Marine Ash Zone (FMAZ) II (see section 2.3), the P-A, B-A, and B-P ventilation ages in the southern Norwegian Sea are  $\sim 1500$ , 2000, and 500  $^{14}\text{C}$  years, respectively (Figure 3). These values are  $\sim 1100$ , 1500, and 400  $^{14}\text{C}$  years higher relative to modern P-A, B-A, and B-P values, respectively. The increase in the B-P ventilation age suggests a reduction in surface-deep mixing, likely related to a decrease in the Arctic Mediterranean overturning circulation. Near the onset of the last deglaciation ( $\sim 20$ –18.5 ka), our results indicate relatively well-ventilated water with P-A  $\sim 500$   $^{14}\text{C}$  years, B-A  $\sim 870$   $^{14}\text{C}$  years, and B-P = 370  $^{14}\text{C}$  years (Figure 3). Although these reconstructions are associated with large errors due to uncertainties in our calendar chronology (Figure 3 and see section 2), they support previous studies [e.g., Crocket *et al.*, 2011; Yu *et al.*, 2008; Howe *et al.*, 2016] that hypothesize active, though weak, Nordic Seas overflows during this time.

During middle and late HS1 (17.5–14.5 ka), our results show substantial differences in the  $^{14}\text{C}$  ventilation ages based on different benthic species (Figure 3). The *Pyrgo* species yield ventilation ages between 6000 and 9000  $^{14}\text{C}$  years, while all other species suggest ventilation ages  $< 2000$   $^{14}\text{C}$  years. In this regard, it is notable that many of the previously published ventilation age reconstructions from the deep Norwegian Sea are based on miliolids, including *Pyrgo* spp. (but notably, not all, two  $^{14}\text{C}$  ventilation ages  $> 6000$   $^{14}\text{C}$  years, from the YD and HS1, were also obtained on *C. wuellerstorfi* [Thornalley *et al.*, 2015]) (Figure 3). *Pyrgo* spp. were also often used in the  $^{14}\text{C}$  ventilation age reconstructions from south of Iceland [Thornalley *et al.*, 2011]. If there is a species-specific offset between *Pyrgo* spp. and perforate benthic foraminifera, and given the typical large size of individual *Pyrgo* spp., inclusion of a few specimens could have a pronounced impact on the obtained radiocarbon dates. Indeed, our new  $^{14}\text{C}$  measurements from sediment core RAPID-10-1P in the Iceland Basin show similar species-specific benthic  $^{14}\text{C}$  age offsets; *Pyrgo* spp. yield B-A ventilation ages  $> 6000$   $^{14}\text{C}$  years, while non-miliolid species and bivalves yield much younger B-A ventilation ages (typically B-A ventilation ages of 1000–3000  $^{14}\text{C}$  years) (Figure 4). Yet samples from RAPID-10-1P that included *Pyrgo* spp. did not always yield older ventilation ages (Figure 4). In the deep Norwegian Sea, Holocene *Pyrgo* and *Cibicides wuellerstorfi* measurements from the same depths yield similar young ages [Thornalley *et al.*, 2015]. Therefore, it is critical to verify and explain these benthic interspecies  $^{14}\text{C}$  age offsets in order to fully understand the deglacial ventilation histories of the high-latitude North Atlantic.

Previous work from the Santa Barbara Basin by Magana *et al.* [2010] also documented anomalously old down-core *Pyrgo*  $^{14}\text{C}$  ages relative to other coeval benthic species (up to 2000 year age offsets). Based on the accompanying low  $\delta^{13}\text{C}$  values ( $-4$  to  $-8\text{‰}$ ), the authors attributed the old  $^{14}\text{C}$  dates measured in *Pyrgo* to the addition of radiocarbon-free hydrocarbon (i.e., tar) to their environment. In contrast, our  $\delta^{13}\text{C}$  measurements in *Pyrgo serrata* show relatively high values ( $=0.6$  to  $0.9\text{‰}$ ) (Table S1 in the supporting information), thus clearly precluding the presence of an isotopically light, e.g., petrogenic carbon source in the calcification environment of *Pyrgo*. Thornalley *et al.* [2015] have also observed similarly high  $\delta^{13}\text{C}$  values in *Pyrgo* species in the deep Norwegian Sea. Also, the sedimentation rates for the investigated sediment cores range from 10 to 60 cm/kyr suggesting insignificant effects of bioturbation on our  $^{14}\text{C}$  ages [e.g., Peng and Broecker, 1984].

Alternative interpretations for very old *Pyrgo*  $^{14}\text{C}$  ages further include (1) upward pumping of coarser components of marine sediments by preferential bioturbation [McCave, 1988], which may have caused large *Pyrgo* specimens to remain close to the surface sediment over long periods of time, resulting in an apparent age

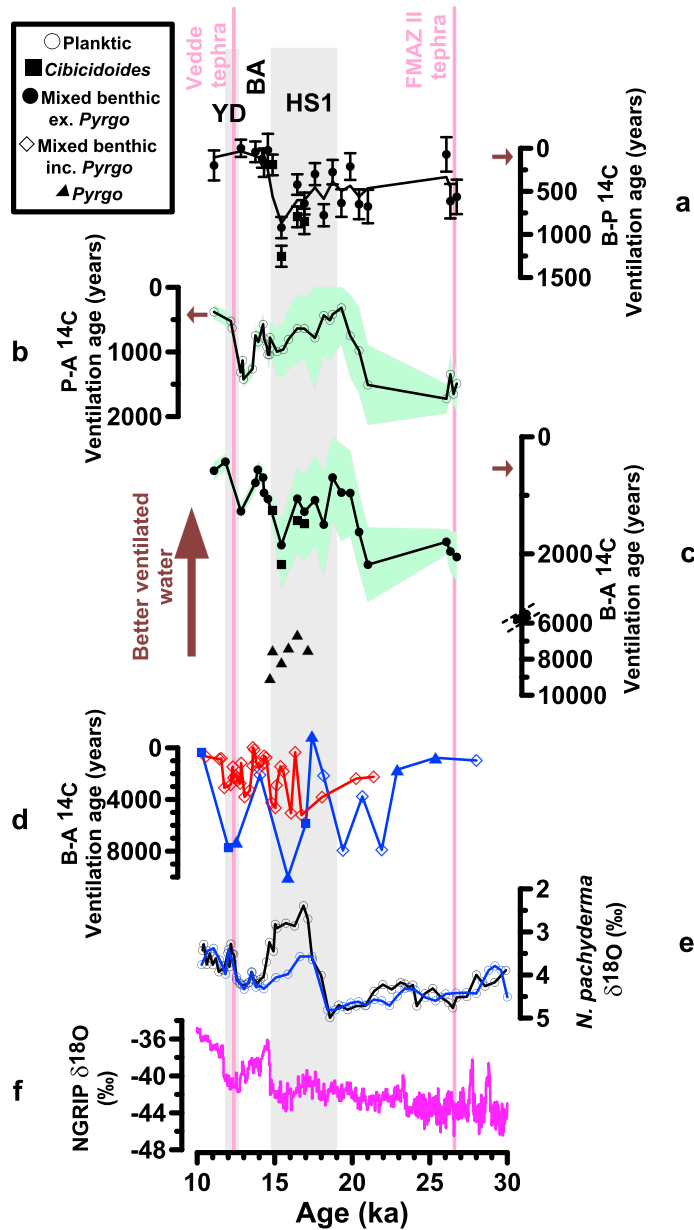


**Figure 3.** Comparison between ventilation age reconstructions of the Norwegian Sea and northern North Atlantic plotted versus Greenland Ice Core Project (NGRIP) Greenland Ice Core Chronology 2005 [Svensson *et al.*, 2008]. (a) Benthos-Plankton (B-P) <sup>14</sup>C age difference reconstructed for the Faroe-Shetland Channel (1179 m water depth). The black line represents 3-point running average. Error bars are combined 1σ errors in planktic and benthic <sup>14</sup>C dates. (b) Plankton-Atmosphere (P-A) ventilation age from the Faroe-Shetland Channel. (c) Benthos-Atmosphere (B-A) ventilation age from the Faroe-Shetland Channel. The solid circles, squares, and triangles indicate B-A ventilation ages based on the “infaunal benthic group” (*Cassidulina neoteretis*, *Melonis barleeanus*, *Elphidium excavatum*, *Oridorsalis umbonatus*, and *Astrononion gallowayi*), the epifaunal *Cibicidoides* spp., and the epifaunal to infaunal *Pyrgo* spp., respectively. Note that we do not present the B-P ventilation ages for the *Pyrgo* spp. in Figure 3a. The green envelope in Figures 3b and 3c reflects the uncertainty boundaries in ventilation ages (see section 2.4). The horizontal brown arrows at the y axes in Figures 3a–3c indicate the modern B-P, P-A, and B-A ventilation age values, respectively. (d) Benthic-Atmosphere (B-A) ventilation age in the deep Norwegian Sea (2700 m water depth; the blue triangles, squares, and open diamonds indicate B-A ventilation ages based on *Pyrgo* spp. (and other miliolid species), *Cibicidoides* spp., and mixed benthic samples (*Cibicidoides* spp. and miliolid species), respectively [Thornalley *et al.*, 2015]) and south of Iceland (1237–2303 m water depth; open red circles [Thornalley *et al.*, 2011]). (e) Planktic δ<sup>18</sup>O measured in *N. pachyderma* from the northern Norwegian Sea (blue open circles [Bauch *et al.*, 2001]) and from the Faroe-Shetland Channel (black open circles [Hoff *et al.*, 2016]). The age model for the sediment record from the northern Norwegian Sea [Thornalley *et al.*, 2015] is slightly modified by aligning it to our sediment record using the start of the deglacial decrease in δ<sup>18</sup>O in *N. pachyderma* as a tuning marker. (f) NGRIP δ<sup>18</sup>O [Svensson *et al.*, 2008, and references therein].

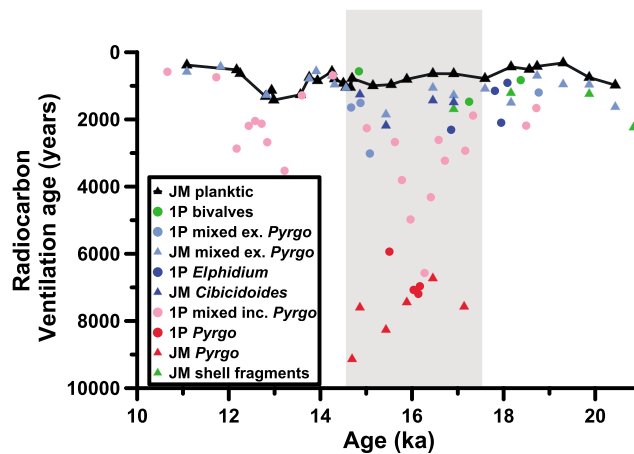


**Figure 4.** Comparison of benthos-atmosphere  $^{14}\text{C}$  age offsets for JM11-FI-19PC (triangles; located in the Faroe Shetland Channel, north of the GSR) and RAPiD-10-1P (circles; located on the South Iceland Rise, south of the GSR). Plankton-Atmosphere ventilation (reservoir) ages from the Faroe-Shetland Channel are also plotted (black line). Radiocarbon dates in RAPiD-10-1P were obtained on either mixed benthic foraminiferal species including (pink circles) or excluding (pale blue circles) *Pyrgo* spp.; paired, intact bivalves (green circles); or monospecific samples of either *Elphidium excavatum* (blue circles), or *Pyrgo serrata* (red circles).

freshwater discharge events during HS1 [Hoff et al., 2016]) will result in high  $\delta^{13}\text{C}$  and depleted  $^{14}\text{C}$  bicarbonate [see Carothers and Kharaka, 1980], it remains elusive why only *Pyrgo* species record the signature of this process. (3) *Pyrgo* specimens may have been transported by either lateral or downslope reworking of older fossil material. Similar extreme old ages of miliolids relative to coeval shells and other benthic foraminifera were also observed from Holocene marine shelf sediments from Skaw Spit, Denmark, and interpreted as miliolids having been laterally entrained from older sediments due to the high-energy environment [Heir-Nielsen et al., 1995]. Yet a similar taphonomic process causing the older  $^{14}\text{C}$  ages obtained on *Pyrgo* and other miliolid species seems implausible for our study, although it cannot be excluded, because of the replication of the interspecies benthic  $^{14}\text{C}$  age offset at two separate sites, JM-FI-19PC and RAPiD-10-1P (~500 km apart, and either side of the GSR) (Figure 4).

Finally, (4) the old  $^{14}\text{C}$  ages recorded by *Pyrgo* in sediment cores JM-FI-19PC and RAPiD-10-1P could indicate intermittent overflow of extremely preaged water from the Arctic Ocean to the North Atlantic [cf. Thornalley et al., 2015]. In this case, the presence of other benthic species that record much younger benthic  $^{14}\text{C}$  ventilation ages at the same sampling depth (each sample is equivalent to tens to several hundreds of years) would require persistent subcentennial fluctuations between the extremely aged overflow and much better ventilated water, coupled with strong habitat differences between different benthic species. The middepth circulation in the modern high-latitude North Atlantic is very dynamic [Hansen and Østerhus, 2000; Eldevik et al., 2009] and is likely to have undergone significant changes on short time scales (decades and shorter) during the deglacial conditions of rapidly melting ice sheets and global warming. Thus, it is plausible that different benthic species dated from the same core depth may record only ephemeral events within the entire period that a sampling depth represents [see Jorissen et al., 2007]. Changes in the benthic foraminiferal fauna may respond to water mass variability directly [e.g., Rasmussen et al., 1996], or possibly indirectly via climatic coupling of middepth oceanographic variability with environmental parameters which alter their food supply (e.g., wind stress and mixing, sea ice cover, and freshwater input) [e.g., Jorissen et al., 2007]. Radiocarbon ventilation ages based on *C. floridanus* or infaunal species other than *Pyrgo* may therefore represent the environmental conditions at times when there were incursions of inflowing subsurface Atlantic water or shallow convection [e.g., Rasmussen et al., 1996; Ezat et al., 2014], whereas *Pyrgo* spp. may instead record times when environmental conditions facilitated the sporadic overflow of extremely aged water. In the deep Norwegian Sea, these very old  $^{14}\text{C}$  ventilation ages are always associated with only a minor depletion in  $\delta^{13}\text{C}$  values (from ~1.5 to 0.8‰) and this absence of significant  $\delta^{13}\text{C}$  depletion has been attributed to decreased primary productivity [Thornalley et al., 2015].

offset and old-biased *Pyrgo*  $^{14}\text{C}$  ages. Although, this may explain some of the  $^{14}\text{C}$  age offsets, it is difficult to explain the entire age offset relative to other benthic species, as this would require a systematic displacement of *Pyrgo* shells by ~1 m from their original growth depth. (2) *Pyrgo* spp. may adopt species-specific “vital effects” under specific environmental conditions (e.g., similar to HS1 hydrography) that would have caused the *Pyrgo*  $^{14}\text{C}$  record to deviate from the ambient seawater  $^{14}\text{C}$  age. If this hypothetical vital effect exists, it does not affect the  $\delta^{13}\text{C}$  signature, which is difficult to conceive [cf. Magana et al., 2010] and remains unsupported by any evidence for *Pyrgo*-specific vital effects. Although microbial fermentation of aged organic matter (which may have been delivered to the site via

Although these findings may pave the way for a more sophisticated approach of using species-specific benthic  $^{14}\text{C}$  analysis to elucidate short-term changes in ocean circulation, it remains uncertain why only *Pyrgo* species, and possibly miliolid species more generally, would tolerate the environmental conditions when the extremely old water recurrently passed our sites for a decade or so over the course of HS1. For example, although *Pyrgo* species are tolerant to very irregular and reduced food supply and thus may persist during short episodes of very low food fluxes [Struck, 1997; Linke and Lutze, 1993], hyaline benthic species such as *Elphidium excavatum* are also well adapted to a very wide range of food supply, temperature, and salinity [Vilks, 1989; Linke and Lutze, 1993]. A possible further challenge to this scenario is also the interpretation of Pa/Th data from the Central Arctic Ocean, which have been used to suggest a centennial scale replacement for deep waters in the Central Arctic Ocean during the past 35 kyr [Hoffmann *et al.*, 2013]; notwithstanding, however, the possibility that boundary scavenging in areas with higher particle fluxes may have been an important sink for Pa [Hoffmann *et al.*, 2013; Luo and Lippold, 2015]. Excluding the miliolid-based  $^{14}\text{C}$  ventilation ages, there is a general trend toward increasing ventilation ages over HS1, reaching maximum values (P-A =  $\sim 800$   $^{14}\text{C}$  years, B-A =  $\sim 1800$   $^{14}\text{C}$  years, and B-P =  $1000$   $^{14}\text{C}$  years) at 15 ka, just prior to the onset of the Bølling-Allerød (BA) interstadial (Figure 3).

At the beginning of the BA interstadial ( $\sim 14.5$  ka), the P-A and B-A ventilation ages decreased to  $\sim 800$  and  $950$   $^{14}\text{C}$  years, respectively. The significant decrease in the B-P ventilation age from  $\sim 400$ – $1000$   $^{14}\text{C}$  years during the glacial and HS1 to  $\sim 105$   $^{14}\text{C}$  years at the onset of the BA interstadials indicates a significant decrease in the apparent stratification between inflowing and outflowing water masses through the Faroe-Shetland Channel. At 14 ka, the P-A, B-A, and B-P ventilation ages reached the modern values, suggesting similar mode and vigor of circulation. Renewal of strong and well-ventilated Nordic Seas overflows would have contributed to the step-change in ocean circulation that has been recorded throughout the Atlantic at this time [McManus *et al.*, 2004; Roberts *et al.*, 2010; Skinner *et al.*, 2014]. During the Intra-Allerød Cold Period (IACP;  $\sim 13.5$ – $12.5$  ka), the P-A and B-A increased significantly to  $\sim 1300$   $^{14}\text{C}$  years. Unfortunately, there were not enough benthic foraminifera in our record to resolve the YD event, only the P-A ventilation ages display an increase of  $200$   $^{14}\text{C}$  years relative to modern (Figure 3b). During the early Holocene (at  $\sim 11$  ka), the P-A, B-A, and B-P ventilation ages are similar to modern values (Figure 3), suggesting that the oceanographic regime was similar to today.

#### 4. Conclusions

The results presented here suggest a similar to modern circulation prevailed in the upper Nordic Seas during warm periods (the Bølling interval and the early Holocene), whereas substantial suppression in the overturning circulation marked cold periods (the late glacial (at  $\sim 26$  ka), late Heinrich Stadial HS1 (at  $\sim 15.5$  ka), and Intra-Allerød Cold period IACP ( $\sim 13.5$ – $12.5$  ka)). During the late LGM and the onset of deglaciation ( $\sim 20$ – $18$  ka), our results suggest active, though weak, Nordic Seas overflows. In addition, our data show that many of the old ventilation ages reconstructed in the glacial and deglacial high-latitude North Atlantic are associated with the use of *Pyrgo* spp. and miliolids, which dated  $\sim 7000$   $^{14}\text{C}$  years older than other coeval benthic species (although it is important to note that old ventilation ages have also been recorded in non-miliolid species (*C. wuellerstorfi*) in the deep Norwegian Sea [Thornalley *et al.*, 2015]). This complicates the interpretation of  $^{14}\text{C}$  ventilation age reconstructions that include *Pyrgo* and miliolid species, since it remains uncertain if these offsets reflect actual differences in past seawater  $^{14}\text{C}$  ventilation, or if they are affected by taphonomic or vital processes. This also implies that the previous reconstructions based on mixed benthic foraminifera (including *Pyrgo* species) of Thornalley *et al.* [2011] may be strongly affected by the relative proportions of different species. We suggest that a critical step toward advancing the use of benthic foraminiferal  $^{14}\text{C}$  ventilation records to examine deglacial circulation in the high-latitude North Atlantic (where hydrography is particularly dynamic) is to consider and investigate benthic interspecies  $^{14}\text{C}$  age offsets, which may have the potential to reveal more detailed hydrographic changes than has hitherto been considered possible.

#### References

- Bauch, H. A., H. Erlenkeuser, R. F. Spielhagen, U. Struck, J. Matthießen, J. Thiede, and J. Heinemeier (2001), A multiproxy reconstruction of the evolution of deep and surface waters in the subarctic Nordic seas over the last 30,000 years, *Quat. Sci. Rev.*, *20*, 659–678.
- Broecker, W. S. (1998), Paleoocean circulation during the last deglaciation: A bipolar seesaw?, *Paleoceanography*, *13*, 119–121, doi:10.1029/97PA03707.
- Broecker, W. S., and T. H. Peng (1982), *Tracers in the Sea*, Eldigio Press, Palisades, New York.

#### Acknowledgments

This research is funded by the Research Council of Norway through its Centres of Excellence funding scheme, project number 223259. M.M. Ezat has also received funding from the Arctic University of Norway and the Mohn Foundation to the Paleo-CIRCUS project. D.J.R.T. is funded by WHOI OCCI grant 27071264. The authors thank J. Sen and N.L. Rasmussen for their help with picking foraminifera and T. Grytå and J. P. Holm for designing the map. We are grateful for the helpful comments of two anonymous reviewers. The data used are listed in the supporting information.



- Burke, A., and L. F. Robinson (2012), The Southern Ocean's role in carbon exchange during the last deglaciation, *Science*, *335*, 557–561.
- Carothers, W. W., and Y. K. Kharaka (1980), Stable carbon isotopes of  $\text{HCO}_3^-$  in oil-field waters—Implications for the origin of  $\text{CO}_2$ , *Geochim. Cosmochim. Acta*, *44*, 323–332.
- Cléroux, C., P. deMenocal, and T. Guilderson (2011), Deglacial radiocarbon history of tropical Atlantic thermocline waters: Absence of  $\text{CO}_2$  reservoir purging signal, *Quat. Sci. Rev.*, *30*, 1875–1882.
- Cook, M. S., and L. D. Keigwin (2015), Radiocarbon profiles of the NW Pacific from the LGM and deglaciation: Evaluating ventilation metrics and the effect of uncertain surface reservoir ages, *Paleoceanography*, *30*, 174–195, doi:10.1002/2014PA002649.
- Crockett, K. C., D. Vance, M. Gutjahr, G. L. Foster, and D. A. Richards (2011), Persistent Nordic deep-water overflow to the glacial North Atlantic, *Geology*, *39*, 515–518.
- Dansgaard, W., S. J. Johnsen, H. B. Clausen, D. Dahl-Jensen, N. S. Gundestrup, C. U. Hammer, C. S. Hvidberg, J. P. Steffensen, A. E. Sveinbjornsdottir, and J. Jouzel (1993), Evidence for general instability of past climate from a 250-kyr ice-core record, *Nature*, *364*, 218–220.
- Davies, S. M., S. Wastegård, T. L. Rasmussen, A. Svensson, S. J. Johnsen, J. P. Steffensen, and K. K. Andersen (2008), Identification of the Fugloyabanki tephra in the NGRIP ice core: A key tie-point for marine and ice-core sequences during the last glacial period, *J. Quat. Sci.*, *23*, 409–414.
- Eldevik, T., J. E. Ø. Nilsen, D. Iovino, K. Anders Olsson, A. Britt Sandø, and H. Drange (2009), Observed sources and variability of Nordic seas overflow, *Nat. Geosci.*, *2*, 406–410.
- European Project for Ice Coring in Antarctica (2006), One-to-one coupling of glacial climate variability in Greenland and Antarctica, *Nature*, *444*, 195–198.
- Ezat, M. M., T. L. Rasmussen, and J. Groenewald (2014), Persistent intermediate water warming during cold stadials in the southeastern Nordic seas during the past 65 k.y., *Geology*, *42*, 663–666.
- Ezat, M. M., T. L. Rasmussen, and J. Groenewald (2016), Reconstruction of hydrographic changes in the southern Norwegian Sea during the past 135 kyr and the impact of different foraminiferal Mg/Ca cleaning protocols, *Geochem. Geophys. Geosyst.*, *17*, 3420–3436, doi:10.1002/2016GC006325.
- Griggs, A. J., S. M. Davies, P. M. Abbott, T. L. Rasmussen, and A. P. Palmer (2014), Optimising the use of marine tephrochronology in the North Atlantic: A detailed investigation of the Faroe Marine Ash Zones II, III, and IV, *Quat. Sci. Rev.*, *106*, 122–139.
- Hansen, B., and S. Østerhus (2000), North Atlantic–Nordic Seas exchanges, *Prog. Oceanogr.*, *45*, 109–208.
- Heir-Nielsen, S., K. Conradsen, J. Heinemeier, K. L. Knudsen, H. L. Nielsen, N. Rud, and A. E. Sveinbjornsdottir (1995), Radiocarbon dating of shells and foraminifera from the Skagen core, Denmark: Evidence of reworking, *Radiocarbon*, *37*, 119–130.
- Hoff, U., T. L. Rasmussen, R. Stein, M. M. Ezat, and K. Fahl (2016), Sea ice and millennial-scale climate variability in the Nordic seas 90 ka to present, *Nat. Commun.*, doi:10.1038/ncomms12247.
- Hoffmann, S. S., J. F. McManus, W. B. Curry, and L. S. Brown-Leger (2013), Persistent export of  $^{231}\text{Pa}$  from the deep central Arctic Ocean over the past 35,000 years, *Nature*, *497*, 603–606.
- Howe, J. N., A. M. Piotrowski, T. L. Noble, S. Mulitza, C. M. Chiessi, and G. Bayon (2016), North Atlantic deep water production during the last glacial maximum, *Nat. Commun.*, *7*.
- Jorissen, F. J., C. Fontanier, and E. Thomas (2007), Paleoclimatological proxies based on deep-sea benthic foraminiferal assemblage characteristics, in *Proxies in Late Cenozoic Paleoclimatology: Pt. 2: Biological Tracers and Biomarkers*, edited by C. Hillaire-Marcel and A. de Vernal, pp. 263–326, Elsevier, Amsterdam.
- Kissel, C., C. Laj, L. Labeyrie, T. Dokken, A. Voelker, and D. Blamart (1999), Rapid climatic variations during marine isotopic stage 3: Magnetic analysis of sediments from Nordic Seas and North Atlantic, *Earth Planet. Sci. Lett.*, *171*, 489–502.
- Linke, P., and G. F. Lutze (1993), Microhabitat preferences of benthic foraminifera—A static concept or a dynamic adaptation to optimize food acquisition?, *Mar. Micropaleontol.*, *20*, 215–234.
- Luo, Y., and J. Lippold (2015), Controls on  $^{231}\text{Pa}$  and  $^{230}\text{Th}$  in the Arctic Ocean, *Geophys. Res. Lett.*, *42*, 5942–5949, doi:10.1002/2015GL064671.
- Magana, A. L., J. R. Southon, J. P. Kennett, E. B. Roark, M. Sarnthein, and L. D. Stott (2010), Resolving the cause of large differences between deglacial benthic foraminifera radiocarbon measurements in Santa Barbara Basin, *Paleoceanography*, *25*, PA4102, doi:10.1029/2010PA002011.
- Mauritzen, C. (1996), Production of dense overflow waters feeding the North Atlantic across the Greenland-Scotland Ridge. Part 1: Evidence for a revised circulation scheme, *Deep Sea Res., Part I*, *43*, 769–806.
- McCave, I. N. (1988), Biological pumping upwards of the coarse fraction of deep-sea sediments, *J. Sediment. Res.*, *58*, 148–158.
- McManus, J. F., R. Francois, J. M. Gherardi, L. D. Keigwin, and S. Brown-Leger (2004), Collapse and rapid resumption of Atlantic meridional circulation linked to deglacial climate changes, *Nature*, *428*, 834–837.
- Meland, M. Y., T. M. Dokken, E. Jansen, and K. Hevrøy (2008), Water mass properties and exchange between the Nordic seas and the northern North Atlantic during the period 23–6 ka: Benthic oxygen isotopic evidence, *Paleoceanography*, *23*, PA1210, doi:10.1029/2007PA001416.
- Monnin, E., A. Indermühle, A. Dällenbach, J. Flückiger, B. Stauffer, T. F. Stocker, D. Raynaud, and J.-M. Barnola (2001), Atmospheric  $\text{CO}_2$  concentrations over the last glacial termination, *Science*, *291*, 112–114.
- Nadeau, M. J., P. M. Grootes, A. Voelker, F. Bruhn, and A. Oriwall (2001), Carbonate  $^{14}\text{C}$  background: Does it have multiple personalities?, *Radiocarbon*, *43*, 169–176.
- Peng, T.-H., and W. Broecker (1984), The impacts of bioturbation on the age difference between benthic and planktonic foraminifera in deep sea sediments, *Nucl. Instrum. Methods Phys. Res.*, *5*, 346–352.
- Rasmussen, T. L., and E. Thomsen (2004), The role of the North Atlantic Drift in the millennial timescale glacial climate fluctuations, *Palaeogeogr. Palaeoclimatol. Palaeoecol.*, *210*, 101–116.
- Rasmussen, T. L., E. Thomsen, L. Labeyrie, and T. C. E. van Weering (1996), Circulation changes in the Faeroe-Shetland Channel correlating with cold events during the last glacial period (58–10 ka), *Geology*, *24*, 937–940.
- Reimer, P. J., et al. (2013), IntCal13 and Marine13 radiocarbon age calibration curves, 0–50,000 years cal BP, *Radiocarbon*, *55*, 1869–1887.
- Richter, T. O., S. van der Gaast, B. Koster, A. Vaars, R. Gieles, H. C. de Stigter, H. De Haas, and T. C. E. van Weering (2006), The Avaatech XRF Core Scanner: Technical description and applications to NE Atlantic sediments, *Geol. Soc. London Spec. Publ.*, *267*, 39–50.
- Roberts, N. L., A. M. Piotrowski, J. F. McManus, and L. D. Keigwin (2010), Synchronous deglacial overturning and water mass source changes, *Science*, *327*, 75–78.
- Sarnthein, M., P. M. Grootes, J. P. Kennett, and M.-J. Nadeau (2007), in *Ocean Circulation: Mechanisms and Impacts*, *Geophys. Monogr. Ser.*, vol. 173, edited by A. Schmittner, J. C. H. Chiang, and S. R. Hemmings, pp. 175–196, AGU, Washington, D. C.
- Shakun, J. D., P. U. Clark, F. He, S. A. Marcott, A. C. Mix, Z. Liu, B. Otto-Bliesner, A. Schmittner, and E. Bard (2012), Global warming preceded by increasing carbon dioxide concentrations during the last deglaciation, *Nature*, *484*, 49–54.

- Sigman, D. M., and E. A. Boyle (2000), Glacial/interglacial variations in atmospheric carbon dioxide, *Nature*, *407*, 859–869.
- Simstich, J., M. Sarnthein, and H. Erlenkeuser (2003), Paired  $\delta^{18}\text{O}$  signals of *Neogloboquadrina pachyderma* (s) and *Turborotalita quinqueloba* show thermal stratification structure in Nordic Seas, *Mar. Micropaleontol.*, *48*, 107–125.
- Skinner, L. C., and N. J. Shackleton (2004), Rapid transient changes in Northeast Atlantic deep-water ventilation-age across Termination I, *Paleoceanography*, *19*, PA2005, doi:10.1029/2003PA000983.
- Skinner, L. C., S. Fallon, C. Waelbroeck, E. Michel, and S. Barker (2010), Ventilation of the deep Southern Ocean and deglacial  $\text{CO}_2$  rise, *Science*, *328*, 1147–1151.
- Skinner, L. C., C. Waelbroeck, A. E. Scrivner, and S. J. Fallon (2014), Radiocarbon evidence for alternating northern and southern sources of ventilation of the deep Atlantic carbon pool during the last deglaciation, *Proc. Natl. Acad. Sci. U.S.A.*, *111*, 5480–5484.
- Sortor, R. N., and D. C. Lund (2011), No evidence for a deglacial intermediate water  $\Delta^{14}\text{C}$  anomaly in the SW Atlantic, *Earth Planet. Sci. Lett.*, *310*, 65–72.
- Soulet, G., L. Skinner, S. R. Beaufre, and V. Galy (2016), A note on reporting of reservoir  $^{14}\text{C}$  disequilibria and Age offsets, *Radiocarbon*, *58*, 205–211.
- Stern, J. V., and L. E. Lisiecki (2013), North Atlantic circulation and reservoir age changes over the past 41,000 years, *Geophys. Res. Lett.*, *40*, 3693–3697, doi:10.1002/grl.50679.
- Struck, U. (1997), Paleoecology of benthic foraminifera in the Norwegian-Greenland Sea during the past 500 ka, *Contrib. Micropaleontology Paleocanogr. Northern North Atlantic*, *5*, 51–82.
- Svensson, A., et al. (2008), A 60 000 year Greenland stratigraphic ice core chronology, *Clim. Past.*, *4*, 47–57.
- Thornalley, D. J. R., H. Elderfield, and I. N. McCave (2010), Intermediate and deep water Paleooceanography of the northern North Atlantic over the past 21,000 years, *Paleoceanography*, *25*, PA1211, doi:10.1029/2009PA001833.
- Thornalley, D. J. R., S. Barker, W. S. Broecker, H. Elderfield, and I. N. McCave (2011), The deglacial evolution of North Atlantic deep convection, *Science*, *331*, 202–205.
- Thornalley, D. J. R., et al. (2015), A warm and poorly ventilated deep Arctic Mediterranean during the last glacial period, *Science*, *349*, 706–710.
- Vilks, G. (1989), Ecology of recent foraminifera on the Canadian continental shelf of the Arctic Ocean, in *The Arctic Seas*, pp. 497–569, Springer.
- Vogel, J. S., J. R. Southon, and D. E. Nelson (1987), Catalyst and binder effects in the use of filamentous graphite for AMS, *Nucl. Instrum. Methods Phys. Res. Section B*, *29*, 50–56.
- Yu, J., H. Elderfield, and A. M. Piotrowski (2008), Seawater carbonate ion- $\delta^{13}\text{C}$  systematics and application to glacial–interglacial North Atlantic ocean circulation, *Earth Planet. Sci. Lett.*, *271*, 209–220.